A Fixed-Point Algorithm for the AC Power Flow Problem

Liangjie (Jeffrey) Chen

Department of Electrical and Computer Engineering
University of Toronto

MASc Oral Defense
September 7, 2022

Background

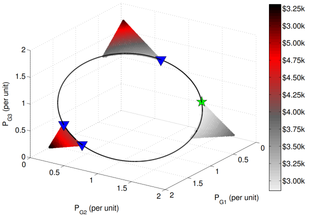

Optimal power flow [1]

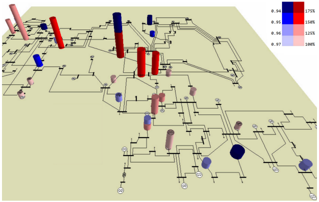

Contingency analysis [2]

Power system expansion [3]

Renewable generation integration [4]

Background

The AC power flow problem

Given a balanced three-phase transmission system at steady-state, compute the bus voltage phasors such that total power generation = total load demand + losses.

- Formulated by a set of <u>nonlinear</u> equations known as the power flow equations

Standard algorithm: Newton-Raphson

- Advantages: simple to implement, fast (quadratic convergence rate)
- Disadvantages: extremely sensitive to initial condition choice, limited theoretical guarantee of convergence

Alternative: fixed-point algorithms

Motivation

Origin of the proposed algorithm: the lossless fixed-point power flow (FPPF) and lossy DC power flow (L-DCPF) [5]–[7]:

- reformulate the power flow equations from the standard $g(\xi) = \mathbb{0}$ form into an equivalent fixed-point form $\xi = f(\xi)$
- start from a ξ_0, iteratively compute $\xi_{k+1} = f(\xi_k)$ until $\|\xi_{k+1} - \xi_k\| \leq \epsilon$
- One example of many other fixed-point based solvability studies/algorithms

Properties of FPPF and L-DCPF:

- highly robust with theoretical guarantees for select system topologies
- restricted to the following simplified contexts
  - FPPF: lossless power flow
  - L-DCPF: decoupled active power flow
- Neither accounts for the existence of nonzero transformer phase-shifts or the distributed slack bus model

Objectives

Practically...

Derive a fixed-point algorithm for the full AC power flow problem, i.e., with **loss**, **coupling** and other transmission system parameters

- fewer simplifying assumptions
- more useful algorithm

Theoretically...

The fixed-point algorithm should allow us to derive sufficient conditions for the existence and uniqueness of the desired power flow solution

- Starting point: 2-bus system (✓)
- Next: radial systems (✗)
- Finally: meshed systems (✗)

Graph modelling of an AC transmission system

Weakly connected bidirected graph

- each node models a bus
  - $\mathcal{N} = \mathcal{N}_L \cup \mathcal{N}_G$: the set of buses
  - $|\mathcal{N}_L| = n$ and $|\mathcal{N}_G| = m$
- each edge models a branch
  - Π-model + transformer
  - $\mathcal{E} = \mathcal{E}^{\ell\ell} \cup \mathcal{E}^{g\ell} \cup \mathcal{E}^{gg}$: the set of edges
- weak connectivity $\Longrightarrow$ number of cycles $n_c = |\mathcal{E}| - (n + m - 1)$
- possibly different forward and backward edge weights w^+, w^-

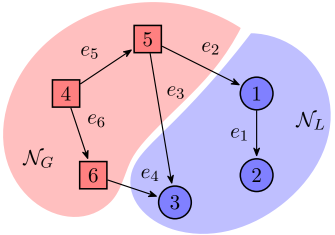

Three important graph matrices

- incidence matrix $A \in \{-1, 0, 1\}^{(n+m)\times|\mathcal{E}|}$
- cycle matrix $C \in \{-1, 0, 1\}^{|\mathcal{E}|\times n_c}$
- asymmetrically weighted incidence matrix $\Gamma \in \mathbb{R}^{(n+m)\times|\mathcal{E}|}$
- important property: $AC = \mathbb{0}$

Branch Modelling

Branch model

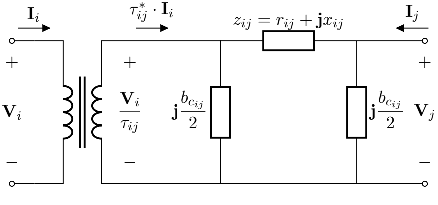

(phase-shifting) transformer + Π-model

$$\begin{bmatrix} \mathbf{I}_i \\ \mathbf{I}_j \end{bmatrix} = \underbrace{\begin{bmatrix} \frac{y_{ij} + \mathbf{j}\frac{b_{c_{ij}}}{2}}{t_{ij}^2} & -\frac{y_{ij}}{\tau_{ij}^*} \\ -\frac{y_{ij}}{\tau_{ij}} & y_{ij} + \mathbf{j}\frac{b_{c_{ij}}}{2} \end{bmatrix}}_{=: Y_{ij}} \begin{bmatrix} \mathbf{V}_i \\ \mathbf{V}_j \end{bmatrix}$$

Bidirected edge model

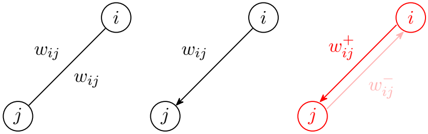

Why asymmetrical edge weights

For the general system with $n + m$ buses...

- We get the G_{ij}, B_{ij} from the off-diagonal entries of $Y = G + \mathbf{j}B$
- Nonzero phase-shift $\implies \tau_{ij} \neq \tau_{ij}^* \implies G_{ij} \neq G_{ji}$ and $B_{ij} \neq B_{ji}$
- Asymmetry $\implies$ need the Γ matrix

The AC Power Flow Problem

The Power Flow Equations w./ Distributed Slack Bus

$$\bar{P}_i + \alpha_i P_{\text{slack}} = \sum_{j=1}^{n+m} \boxed{V_i V_j G_{ij}} \boxed{\cos(\theta_i - \theta_j)} + \boxed{V_i V_j B_{ij}} \boxed{\sin(\theta_i - \theta_j)} \qquad i \in \mathcal{N}$$

$$Q_i = \sum_{j=1}^{n+m} \boxed{V_i V_j G_{ij}} \boxed{\sin(\theta_i - \theta_j)} - \boxed{V_i V_j B_{ij}} \boxed{\cos(\theta_i - \theta_j)} \qquad i \in \mathcal{N}_L$$

Known Variables

- Power injection: $\bar{P}_i \;\; \forall i \in \mathcal{N}$ and $Q_i \;\; \forall i \in \mathcal{N}_L$
- Participation factor: $\alpha_i \;\; \forall i \in \mathcal{N}$
- Gen. voltage mag.: $V_i \;\; \forall i \in \mathcal{N}_G$
- Admittance: $G_{ij} + \mathbf{j}B_{ij} \;\; \forall (i,j) \in \mathcal{E}$

Unknown Variables

- Bus voltage phase: $\theta_i \;\; \forall i \in \mathcal{N}$
- Load voltage mag.: $V_i \;\; \forall i \in \mathcal{N}_L$
- Gen. reactive power injection: $Q_i \;\; \forall i \in \mathcal{N}_G$
- Total network loss: $P_{\text{slack}} \geq 0$

Vectorizing the Power Flow Equations I: Voltage Products

Partitioned variables

$$V = \left[\begin{array}{c} V_L \\ \hline V_G \end{array}\right]$$

$$B = \mathrm{Im}\{Y\} = \left[\begin{array}{c|c} B_{LL} & B_{LG} \\ \hline B_{GL} & B_{GG} \end{array}\right]$$

Open-circuit voltage magnitude

$$V_L^\circ = -B_{LL}^{-1} B_{LG} V_G, \quad V^\circ = \begin{bmatrix} V_L^\circ \\ V_G \end{bmatrix}$$

Normalized voltage magnitudes

$$v = [V_L^\circ]^{-1} V_L, \quad g(v) = \begin{bmatrix} v \\ \mathbb{1}_m \end{bmatrix}$$

Handling voltage products $V_i V_j$ using the incidence matrix A

Let $A = A^+ - A^-$. For all forward edge $(i,j) \in \mathcal{E}$,

$$h_{(i,j)}(v) := \begin{cases} v_i v_j & \text{if } (i,j) \in \mathcal{E}^{\ell\ell} \\ v_j & \text{if } (i,j) \in \mathcal{E}^{g\ell} \\ 1 & \text{if } (i,j) \in \mathcal{E}^{gg} \end{cases} \implies h(v) := \left[\left(A^+\right)^{\mathsf{T}} g(v)\right] \left(A^-\right)^{\mathsf{T}} g(v)$$

Vectorizing the Power Flow Equations II: Admittance

- Nonzero transformer phase-shift $\implies$ $G_{ij} \neq G_{ji}, B_{ij} \neq B_{ji}$
- Need to incorporate both G_{ij}, G_{ji} and B_{ij}, B_{ji} depending on whether (i,j) or (j,i) is the forward edge

Branch stiffness matrices

$$D_G^+ = \left[V_i^\circ V_j^\circ G_{ij}\right]_{(i,j)\in\mathcal{E}}$$

$$D_G^- = \left[V_i^\circ V_j^\circ G_{ji}\right]_{(i,j)\in\mathcal{E}}$$

$$D_B^+ = \left[V_i^\circ V_j^\circ B_{ij}\right]_{(i,j)\in\mathcal{E}}$$

$$D_B^- = \left[V_i^\circ V_j^\circ B_{ji}\right]_{(i,j)\in\mathcal{E}}$$

Handling $V_i V_j G_{ij}, V_i V_j B_{ij}$ products

$$[V_i V_j G_{ij}]_{(i,j)\in\mathcal{E}} = D_G^+[h(v)]$$

$$[V_i V_j B_{ij}]_{(i,j)\in\mathcal{E}} = D_B^+[h(v)]$$

$$[V_i V_j G_{ji}]_{(i,j)\in\mathcal{E}} = D_G^-[h(v)]$$

$$[V_i V_j B_{ji}]_{(i,j)\in\mathcal{E}} = D_B^-[h(v)]$$

Branch quantity to bus quantity

$$\Gamma_B := A^+ D_B^+ - A^- D_B^- \qquad |\Gamma_B| := A^+ D_B^+ + A^- D_B^-$$

$$\Gamma_G := A^+ D_G^+ - A^- D_G^- \qquad |\Gamma_G| := A^+ D_G^+ + A^- D_G^-$$

Vectorizing the Power Flow Equations III

Handling the sinusoidal terms

- Branch-wise phase difference $\theta_i - \theta_j \implies$ vectorized by $A^\mathsf{T}\theta$
- $\cos(\theta_i - \theta_j) \implies \mathbf{cos}(A^\mathsf{T}\theta)$, $\sin(\theta_i - \theta_j) \implies \mathbf{sin}(A^\mathsf{T}\theta)$ (!)

Handling the loss P_{slack}

- Known participation factors $\alpha_i \geq 0, \quad \forall i \in \mathcal{N}$

$$\alpha := \begin{bmatrix} \mathbb{0} \\ \hline \alpha_G \end{bmatrix} \implies \exists R \in \mathbb{R}^{(n+m)\times(n+m-1)} \text{ s.t. } \begin{cases} \operatorname{rank}(R) = n + m - 1 \\ R^\mathsf{T}\alpha = \mathbb{0} \end{cases}$$

Vectorized Power Flow Equations

$$\begin{aligned} R^\mathsf{T}\bar{P} &= R^\mathsf{T}[V^\circ][g(v)][G_{ii}][V^\circ]g(v) \qquad M_B := R^\mathsf{T}\Gamma_B \\ &\quad + R^\mathsf{T}|\Gamma_G|[h(v)]\mathbf{cos}(A^\mathsf{T}\theta) + \boxed{M_B}[h(v)]\mathbf{sin}(A^\mathsf{T}\theta) \\ Q_L &= -[V_L^\circ][v][B_{ii}]_L[V_L^\circ]v + \Gamma_{G_L}[h(v)]\mathbf{sin}(A^\mathsf{T}\theta) - |\Gamma_{B_L}|[h(v)]\mathbf{cos}(A^\mathsf{T}\theta) \end{aligned}$$

Fixed-Point Reformulation I: Active Power Flow Eq's

Change of variables

- $\psi := \sin(A^\mathsf{T}\theta) \implies \cos(A^\mathsf{T}\theta) = \sqrt{\mathbb{1} - [\psi]\psi} =: \eta$
- Must have $\|\psi\|_\infty \leq 1$

Vectorized active power flow equation

$$R^\mathsf{T}\bar{P} = R^\mathsf{T}\left([V^\circ][g(v)][G_{ii}][V^\circ]g(v) + |\Gamma_G|[h(v)]\eta\right) + M_B[h(v)]\psi$$

Lemma 4.1

If all off-diagonal entries of B are strictly positive (Asm. 2.2), then M_B has a right inverse $M_B^\dagger$ such that $M_B M_B^\dagger = I$.

Fixed-point active power flow equation

$$\psi = \underbrace{[h(v)]^{-1}M_B^\dagger R^\mathsf{T}\left(\bar{P} - [V^\circ][g(v)][G_{ii}][V^\circ]g(v) - |\Gamma_G|[h(v)]\eta\right)}_{\text{particular soln.}} + \underbrace{[h(v)]^{-1}Kx_c}_{\text{hom. soln.}}$$

- ψ is a function of v, η and x_c

Fixed-Point Reformulation II: Loop Flow Constraint

To recover θ from ψ:

$$\psi = \mathbf{sin}(A^\mathsf{T}\theta) = \mathbf{sin}(A^\mathsf{T}\theta + 2\pi k),\ k \in \mathbb{Z}$$

Key property of the cycle matrix C:

$$AC = \mathbb{0} \implies C^\mathsf{T} A^\mathsf{T}\theta = C^\mathsf{T}\mathbf{arcsin}(\psi) = \mathbb{0}$$

Consequence: loop flow constraint

$$C^\mathsf{T}\mathbf{arcsin}(\psi) \bmod 2\pi = \mathbb{0}$$

The cycle slack variable x_c in ψ must satisfy this constraint!

Solving for x_c

- Constraint already in root-finding form
- Newton-Raphson: $x_c^{k+1} = x_c^k - \left(J_c^k\right)^{-1} C^\mathsf{T}\mathbf{arcsin}(\psi)$

Fixed-Point Reformulation III: Reactive Power Flow Eq's

Vectorized reactive power flow equation

$$Q_L = -[V_L^\circ][v][B_{ii}]_L[V_L^\circ]v + \Gamma_{G_L}[h(v)]\psi - |\Gamma_{B_L}|[h(v)]\eta$$

- $\eta := \sqrt{\mathbb{1} - [\psi]\psi}$

Nodal Stiffness Matrix

$$S := \frac{1}{4}[V_L^\circ]B_{LL}[V_L^\circ]$$

- (Asm. 2.1) B_{LL} invertible
- S invertible

Consequence of Lemma 4.2

$$-[V_L^\circ][v][B_{ii}]_L[V_L^\circ]v - |\Gamma_{B_L}|[h(v)]\mathbb{1}_{|\mathcal{E}|} = 4[v]S(\mathbb{1}_n - v)$$

Fixed-point reactive power flow equation

$$v = \mathbb{1}_n - \frac{1}{4}S^{-1}[v]^{-1}\left(Q_L - \Gamma_{G_L}[h(v)]\psi - |\Gamma_{B_L}|[h(v)]\left(\mathbb{1}_{|\mathcal{E}|} - \eta\right)\right)$$

Fixed-Point Reformulation IV: Main Result

Theorem 4.1

If Assumptions 2.1–2.2 hold, then the following statements are equivalent:

- (V_L, θ) solves the vectorized power flow equations

$$
\begin{aligned}
R^{\mathsf{T}}\bar{P} &= R^{\mathsf{T}}[V^{\circ}][g(v)][G_{ii}][V^{\circ}]g(v) \\
&\quad + R^{\mathsf{T}}|\Gamma_G|[h(v)]\mathbf{cos}(A^{\mathsf{T}}\theta) + M_B[h(v)]\mathbf{sin}(A^{\mathsf{T}}\theta) \\
Q_L &= -[V_L^{\circ}][v][B_{ii}]_L[V_L^{\circ}]v + \Gamma_{G_L}[h(v)]\mathbf{sin}(A^{\mathsf{T}}\theta) - |\Gamma_{B_L}|[h(v)]\mathbf{cos}(A^{\mathsf{T}}\theta)
\end{aligned}
$$

- (v, ψ, x_c) satisfy

Fixed-point eq's for (v, ψ)

$$
\boxed{
\begin{aligned}
v &= \mathbb{1}_n - \frac{1}{4}S^{-1}[v]^{-1}\left(Q_L - \Gamma_{G_L}[h(v)]\psi - |\Gamma_{B_L}|[h(v)]\left(\mathbb{1}_{|\mathcal{E}|} - \eta\right)\right) \\
\psi &= [h(v)]^{-1}M_B^{\dagger}R^{\mathsf{T}}\left(\bar{P} - [V^{\circ}][g(v)][G_{ii}][V^{\circ}]g(v) - |\Gamma_G|[h(v)]\eta\right) \\
&\quad + [h(v)]^{-1}Kx_c
\end{aligned}
}
$$

$$
\boxed{\mathbb{0}_{n_c} = C^{\mathsf{T}}\mathbf{arcsin}(\psi) \bmod 2\pi}
$$

Loop-flow constraint for x_c

where $\eta := \sqrt{\mathbb{1} - [\psi]\psi}$.

Two-Bus Power Flow I: Preliminaries

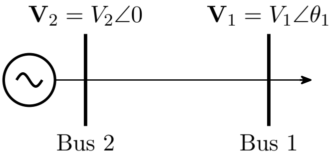

One-line diagram of the two-bus system; transformer tap ratio $\tau = t\exp(\mathbf{j}\theta_s)$ and transmission line parameters g, b, b_c not shown

Two-bus system constants

- $\bar{t} := t - 1$
- $\tilde{g} := \dfrac{g\cos\theta_s - b\sin\theta_s}{\bar{t}+1}$
- $\tilde{b} := \dfrac{b\cos\theta_s + g\sin\theta_s}{\bar{t}+1}$
- $\hat{b} := b - \dfrac{b_c}{2}$
- $\rho := g/\hat{b}$
- $\tilde{\rho} := \tilde{g}/\tilde{b}$
- $\tilde{\gamma}_P := \dfrac{\bar{P}_1}{\tilde{b}V_1^\circ V_2^\circ}$
- $\tilde{\gamma}_Q := \dfrac{Q_1}{\tilde{b}V_1^\circ V_2^\circ}$

FPPF algorithm update rule

$$\xi_{k+1} = F_\mu(\xi_k) = \begin{bmatrix} \dfrac{-\tilde{\gamma}_P}{x_k+1} + \rho\,(x_k+1) - \tilde{\rho}\sqrt{1-\psi_k^2} \\ \dfrac{\tilde{\gamma}_Q}{x_k+1} - \tilde{\rho}\psi_{k+1} + \sqrt{1-\psi_{k+1}^2} - 1 \end{bmatrix} = \begin{bmatrix} \psi_{k+1} \\ x_{k+1} \end{bmatrix} = \begin{bmatrix} \psi_{k+1} \\ v_{k+1} - 1 \end{bmatrix}$$

- Perturbation vector $\mu = [g \quad b_c \quad \bar{t} \quad \theta_s]^\mathsf{T}$

Two-Bus Power Flow II: The Nominal Case ($\mu = \mathbb{0}$)

Loading margin and constants

- $\tilde{\gamma}_P, \tilde{\gamma}_Q \implies \gamma_P, \gamma_Q$
- Asm. 5.2: $0 < \gamma_P^2 - \gamma_Q < \frac{1}{4}$
- $k_2^- := 1 - \sqrt{\frac{1}{2} + \gamma_Q + \sqrt{\frac{1}{4} + \gamma_Q - \gamma_P^2}}$
- $k_1^- := -\dfrac{\gamma_P}{1 - k_2^-}$

FPPF update rule

- $\mu = \mathbb{0}$: $F_\mu \implies F_{\mathbb{0}}$

$$\xi_{k+1} := \underbrace{\begin{bmatrix} -\dfrac{\gamma_P}{x_k + 1} \\ \dfrac{\gamma_Q}{x_k + 1} + \sqrt{1 - \psi_{k+1}^2} - 1 \end{bmatrix}}_{F_{\mathbb{0}}(\xi_k)}$$

Nominal system results (Theorems 5.1-5.2, Corollary 5.1)

If Asm. 5.2 holds, then

- $\mathcal{A}^- := \{\xi : |\psi| \le k_1^-, |x| \le k_2^-\}$ is $F_{\mathbb{0}}$-invariant
- $F_{\mathbb{0}}$ is a contraction on $\mathcal{A}^-$
- High-voltage soln.: $\bar{\xi}^+ = [k_1^- \ \ -k_2^-]^\mathsf{T} \in \mathcal{A}^-$

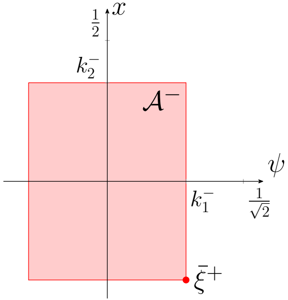

Two-Bus Power Flow III: The Full Case ($\mu \neq \mathbb{0}$)

The F_μ-invariant set $\mathcal{A}_\epsilon^-$

- Constructed using $\mathcal{A}^-$ with additional constants $\epsilon = (\epsilon_1, \epsilon_2) > \mathbb{0}$

$$\mathcal{A}_\epsilon^- := \{\xi : |\psi| \leq k_1^- + \epsilon_1, |x| \leq k_2^- + \epsilon_2\}$$

- Propositions 5.1-5.2: if μ is sufficiently small, then there exists $\epsilon > \mathbb{0}$ such that $\mathcal{A}_\epsilon^-$ is F_μ-invariant

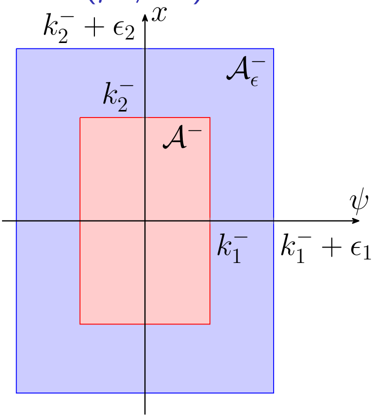

Full system results

For sufficiently small μ, $F_\mathbb{0}$ is a contraction on $\mathcal{A}_\epsilon^-$, so

- the unique high-voltage soln. is in $\mathcal{A}_\epsilon^-$
- FPPF always converges to this soln. from any $\xi_0 \in \mathcal{A}_\epsilon^-$

Numerical Results I: Convergence

Numerical Results I: Convergence

Number of iterations required for convergence

	Base loading			High loading		
Test case	NR	FDLF	FPPF	NR	FDLF	FPPF
9 bus system	4	6	8	5	29	22
30 bus system	3	11	18	6	28	22
PEGASE 89	4	9	10	6	26	23
118 bus system	4	11	11	6	33	25
300 bus system	5	15	33	6	33	33
PEGASE 1354	5	11	42	5	25	42
RTE 1888	/	61	33	/	76	33
RTE 1951	/	55	32	/	58	32
RTE 2868	/	49	43	/	46	44
PEGASE 2869	5	11	42	6	29	42
PEGASE 9241	6	17	46	6	23	47

Numerical Results II: Effect of R/X Ratio

System data: distribution of branch R/X ratios

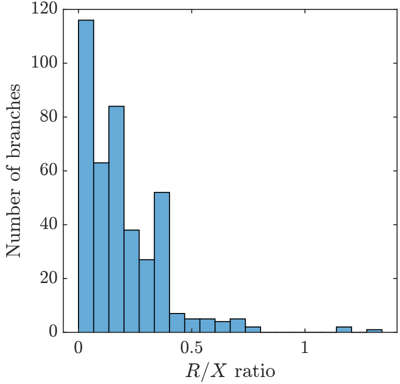

300 bus system

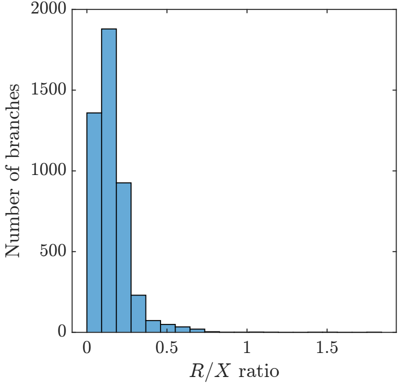

PEGASE 2869 bus system

Number of branches with high R/X ratio

- 300 bus system: 3 out of 411 total branches
- PEGASE 2869 system: 5 out of 4582 total branches

Numerical Results II: Effect of R/X Ratio

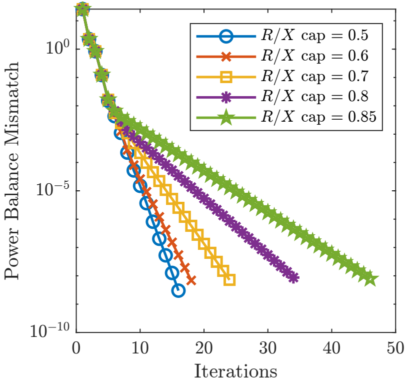

300 bus system; mismatch

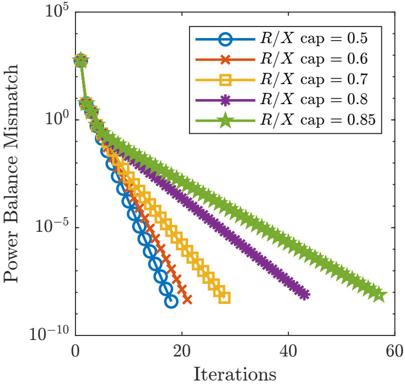

PEGASE 2869 bus system; mismatch

- Iterations required to converge $\uparrow$ as R/X ratio cap $\uparrow$
- Algorithm fails when the cap is too high (1.00 for 300 bus system and 1.01 for 2869 bus system)

Numerical Results III: Sensitivity to Initialization

- **Goal**: test algorithm success rate (%) under random initial load bus voltage magnitudes, generated uniformly from $[1-\delta, 1+\delta]$
- Higher success rate as δ increases $\implies$ more robust

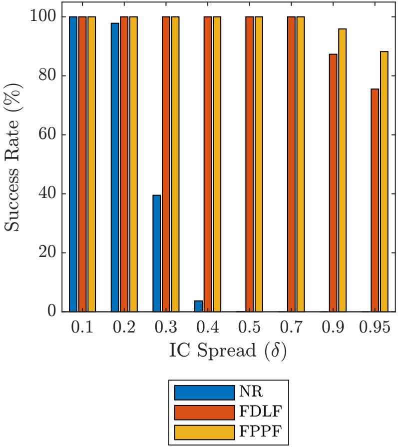

30 bus system, high loading

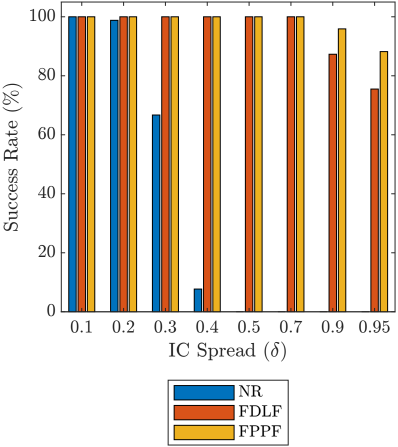

118 bus system, high loading

Conclusions

A new fixed-point algorithm for the AC power flow problem

- Extends the lossless FPPF & L-DCPF algorithms in the literature
- Allows phase-shifting transformers & distributed slack bus setup in the system
- More robust against initial voltage magnitude variations than NR, FDLF

A framework to study the solvability of the full power flow equations

- Bidirected graph model accomodates realistic transmission line and transformer parameters
- Sufficient conditions for two-bus power flow solvability, using the language of invariance sets and contraction mapping

Future Work

Practically

- Optimize the implementation of the algorithm
- Further investigate the effect of high branch R/X ratio on the algorithm convergence/divergence
- Investigate the causes of the $\|\psi\|_\infty \leq 1$ constraint violation

Theoretically

- Potentially revise the fixed-point reformulation to explicitly include R/X information
- Generalize the two-bus power flow solvability conditions to N-bus systems
- Produce tighter and/or constructive sufficient solvability conditions for the two-bus power flow problem

The End

Thank you!

Bibliography I

[1] D. K. Molzahn, "Computing the feasible spaces of optimal power flow problems," *IEEE Transactions on Power Systems*, vol. 32, no. 6, pp. 4752–4763, 2017. DOI: 10.1109/TPWRS.2017.2682058.

[2] Y. Sun and T. Overbye, "Visualizations for power system contingency analysis data," *IEEE Transactions on Power Systems*, vol. 19, no. 4, pp. 1859–1866, 2004. DOI: 10.1109/TPWRS.2004.836193.

[3] J. J. Love, E. J. Rigler, A. Pulkkinen, and C. C. Balch, *Magnetic storms and induction hazards*, https://eos.org/features/magnetic-storms-induction-hazards, Accessed: 2022-08-20, Dec. 2014.

[4] T. Ledbetter, *This dispatch delivers good energy news*, https://www.pnnl.gov/news-media/dispatch-delivers-good-energy-news, Aug. 2019.

Bibliography II

[5] J. W. Simpson-Porco, "A theory of solvability for lossless power flow equations – Part I: Fixed-point power flow," *IEEE Transactions on Control of Network Systems*, vol. 5, no. 3, pp. 1361–1372, 2018.

[6] J. W. Simpson-Porco, "A theory of solvability for lossless power flow equations – Part II: Conditions for radial networks," *IEEE Transactions on Control of Network Systems*, vol. 5, no. 3, pp. 1373–1385, 2018.

[7] J. W. Simpson-Porco, "Lossy DC power flow," *IEEE Transactions on Power Systems*, vol. 33, no. 3, pp. 2477–2485, 2018.